

Journal of Materials Chemistry A

Accepted Manuscript



This is an *Accepted Manuscript*, which has been through the Royal Society of Chemistry peer review process and has been accepted for publication.

Accepted Manuscripts are published online shortly after acceptance, before technical editing, formatting and proof reading. Using this free service, authors can make their results available to the community, in citable form, before we publish the edited article. We will replace this *Accepted Manuscript* with the edited and formatted *Advance Article* as soon as it is available.

You can find more information about *Accepted Manuscripts* in the [Information for Authors](#).

Please note that technical editing may introduce minor changes to the text and/or graphics, which may alter content. The journal's standard [Terms & Conditions](#) and the [Ethical guidelines](#) still apply. In no event shall the Royal Society of Chemistry be held responsible for any errors or omissions in this *Accepted Manuscript* or any consequences arising from the use of any information it contains.

Highlight Article for Journal of Materials Chemistry A

Polymerized Ionic Liquid Block Copolymers for Electrochemical Energy

*Kelly M. Meek, Yossef A. Elabd **

Department of Chemical Engineering, Texas A&M University, College Station, TX 77843

* Corresponding author; E-mail: elabd@tamu.edu

ABSTRACT: Polymerized ionic liquid (PIL) block copolymers are an emerging class of polymers that synergistically combine the benefits of both ionic liquids (ILs) and block copolymers into one, where the former possesses a unique set of physiochemical properties and the latter self assembles into a range of nanostructures. The potential to synthesize a vast array of new block copolymers is almost limitless with numerous IL cations and anions available. In this paper, we highlight the very recent work on PIL block copolymers, specifically, synthesis and unique solid-state properties for electrochemical energy.

Introduction

Ionic liquids (ILs) are salts composed of an organic cation and an organic or inorganic anion, which typically have a melting point below 100 °C; they are also referred to as room temperature ionic liquids (RTILs), when the melting point is below room temperature. ILs possess unique physiochemical properties, such as negligible vapor pressure, non-flammability, a wide electrochemical window, high ionic conductivity, high chemical and thermal stability, and a broad chemical diversity owing to a large number of cations and anions available that can form ILs. These properties along with their ability to be used as green solvents for synthesis and

catalysis¹ have led to a high concentration of research over the past 15-20 years, long after the first IL was reported by Walden² over 100 years ago. In particular, the unique electrochemical properties of ILs have attracted interest for use in electrochemical energy devices, such as fuel cells and batteries.³

In 1998, Ohno⁴ reported on the first polymerized ionic liquid (PIL): a polymeric form of an IL, where the cations of the IL are covalently attached to each monomeric unit of the polymer chain and are neutralized by mobile anions. Unlike other ion-containing polymers that are typically constrained to high glass transition temperatures due to strong electrostatic ion pair interactions, PILs can possess low glass transition temperatures due to weak electrostatic ion pair interactions, while maintaining high charge densities.⁵

This set of new ion-containing polymers, with a broad range of properties due to their chemical diversity, have garnered a significant amount of publications over the past decade, which have been reviewed by several research groups.⁶⁻¹⁰ Unlike ILs where both cations and anions are mobile in a liquid phase, polymerization of an IL monomer results in a single-ion (anion) conductor, because the cations are covalently attached to the polymer chain. This can have a variety of implications as it applies to components (*e.g.*, solid-state electrolytes and electrodes) in electrochemical energy devices.

Electrochemical devices require robust electrolyte films; due to the limited range of mechanical properties of PIL homopolymers, a new material has recently evolved from this class referred to as PIL block copolymers. PIL block copolymers are a distinct set of block copolymers that combine the properties of both ILs and block copolymers, where the resulting material can possess orthogonal properties, such as high modulus (from the non-ionic polymer) and high conductivity (from the ionic polymer or PIL) through the self-assembly of two distinct polymers

into well-defined nanostructures of long-range order (*e.g.*, body-centered-cubic spheres, hexagonal cylinders, bicontinuous gyroid, lamellae) with tunable morphology and domain size. An example chemical structure of a PIL block copolymer is shown in Figure 1 including a variety of typical cations and anions that have been investigated, where, to date, imidazolium has been the most frequently explored cation. The first PIL block copolymer was reported by Waymouth, Gast, and coworkers^{11, 12} in 2004. More recently, there has been an increasing number of publications on PIL block copolymers.¹³⁻⁴⁷ Although some block copolymers containing covalently attached ammonium cations can be classified as PIL block copolymers, they have typically not been referred to as PIL block copolymers in the literature and therefore are not discussed in detail in this paper.

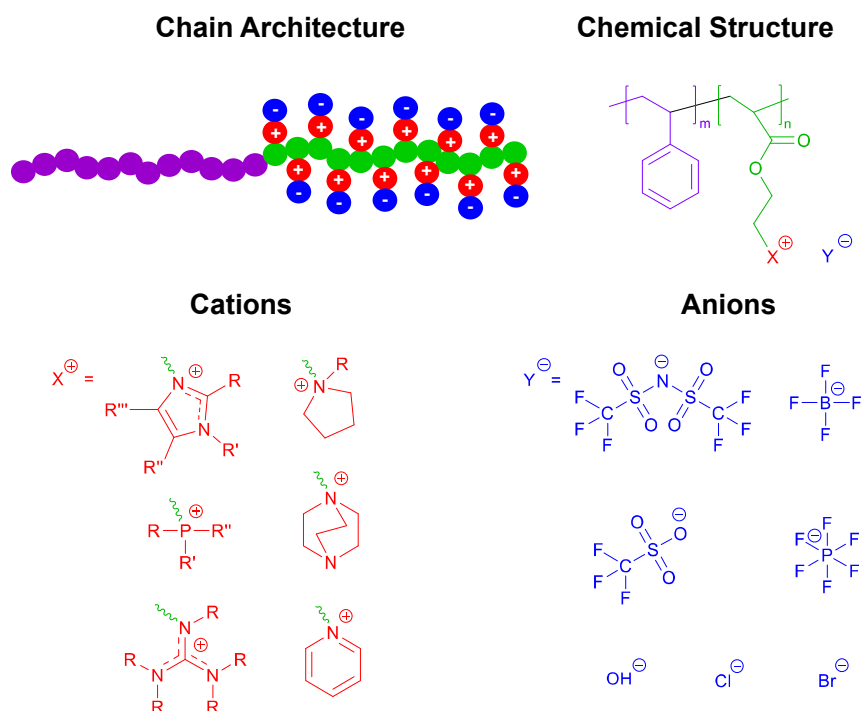


Fig. 1 PIL block copolymer: (upper left) illustration of polymer chain architecture, (upper right) example chemical structure, (lower left) example cations, (lower right) example anions.

To date, investigators have explored the solution properties of PIL block copolymers, such as micelle behavior^{11, 12, 21, 22, 26, 28, 44} and stimuli-responsive behavior,^{22, 23, 26, 28, 44} and solid-state properties, such as ion and gas transport,^{13-16, 18, 24, 25, 27, 30, 34, 37, 38, 43} thermo-mechanical properties,¹⁶ and magnetic properties.^{20, 33} A key interest in PIL block copolymers is not only the combination of PIL and block copolymer properties in one material, but also the ability to significantly impact properties through subtle chemical changes (*e.g.*, *via* anion exchange). In this paper, we will highlight the recent work on PIL block copolymers, specifically, their synthesis and unique solid-state properties, as it applies to electrochemical energy.

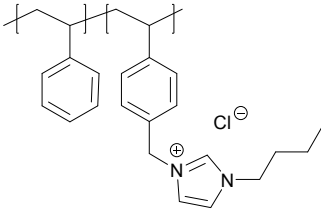
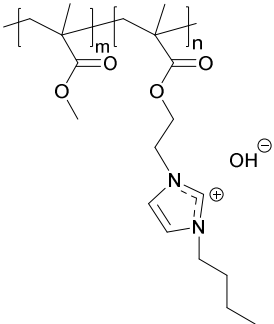
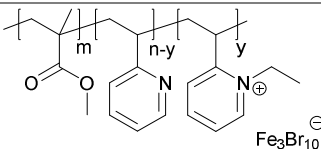
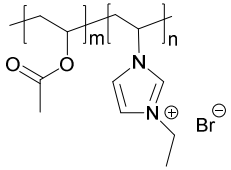
2. Discussion

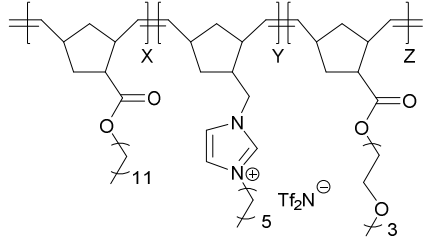
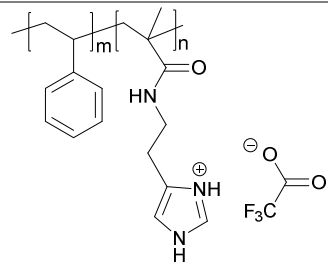
2.1. Synthesis

Table 1 lists various controlled polymerization techniques (*e.g.*, NMP, RAFT, anionic, CMRP, ROMP, ATRP) that have recently been explored to prepare PIL block copolymers.¹¹⁻⁴⁷ Within these techniques, generally two overarching strategies have been used to produce PIL block copolymers: the sequential polymerization of multiple non-ionic monomers followed by subsequent functionalization or quaternization of one of the monomers^{11, 12, 14, 27, 30-34, 42, 43} and the direct sequential polymerization of a non-ionic monomer and an IL monomer.^{13, 15-26, 28, 29, 35-41, 44-47} The former allows for facile molecular weight determination of the non-ionic precursor block copolymer with conventional techniques, such as gel permeation chromatography (GPC). The latter requires the addition of salt to minimize the aggregation of the charged polymer in solution when using techniques such as GPC.^{5, 48, 49} For both strategies, a wide range of cations and anions can be explored, where a variety of anions can easily be accessed *via* simple ion

exchange of the PIL block copolymer. Here, we briefly highlight various chemistries from each of the polymerization techniques shown in Table 1.

Table 1 Examples of PIL block copolymers and their polymerization techniques

Polymerization Techniques	Example Structures	References	Additional References
Nitroxide-mediated polymerization (NMP)		13	11, 12, 14-17
Reversible addition-fragmentation chain transfer (RAFT)		18, 19	20-32
Anionic		33	34
Cobalt-mediated radical polymerization (CMRP)		35	36

Ring opening metathesis polymerization (ROMP)		37	38-42
Atom transfer radical polymerization (ATRP)		43	44-47

Nitroxide-mediated free radical polymerization (NMP) has been used to synthesize several PIL block copolymers.¹¹⁻¹⁷ In fact in 2004, the first PIL block copolymer was synthesized *via* NMP by Waymouth, Gast, and coworkers.^{11, 12} In this study, NMP was used to polymerize styrene and subsequently grow poly(chloromethylstyrene) (PCMS), followed by post-functionalization with 1-methylimidazole and anion exchange from chloride (Cl^-) to tetrafluoroborate (BF_4^-). Recently, Balsara and coworkers¹³ (see structure in Table 1) and others^{14, 16} have reported on the synthesis of PIL diblock copolymers similar to Waymouth, Gast, and coworkers^{11, 12} with a variety of cations and anions. Recently, Long and coworkers¹⁵ were the first to report on the synthesis of a phosphonium-containing PIL triblock copolymer using NMP from the polymerization of a phosphonium-based ionic liquid monomer.

Reversible addition-fragmentation chain transfer (RAFT) polymerization has been the most frequently used technique for producing PIL block copolymers.¹⁸⁻³² Mecerreyes, Taton, Gnanou, *et al.*²¹ reported on the first use of RAFT to synthesize a PIL block copolymer. More recently, Elabd, Winey, and coworkers^{18, 19, 25} synthesized imidazolium-containing methacrylate-based

PIL block copolymers at various compositions by first polymerizing methyl methacrylate (MMA) as the macro chain transfer agent (macro-CTA), followed by copolymerization with an ionic liquid methacrylate monomer with a tethered butylimidazolium (BIm^+) cation and mobile bromide (Br^-) anion. In the resulting PIL block copolymer, poly(MMA-*b*-MEBIm-Br), Br^- was ion exchanged to other anions, such as the fluorinated anion bis((trifluoromethyl)sulfonyl)-imide (TFSI)²⁵ as well as the hydrophilic anion hydroxide (OH^-) (see structure in Table 1).^{18, 19} Elabd, Winey, and coworkers²⁷ also produced a similar PIL block copolymer, where the non-ionic block was styrene instead of MMA and the imidazolium-based cation was tethered via post-functionalization of the non-ionic precursor block copolymer instead of polymerization of the IL monomer. Similarly, Balsara and coworkers³⁰ used RAFT to synthesize a styrene-based PIL block copolymer with a phosphonium-based cation.

Garcia and coworkers^{33, 34} used anionic polymerization to synthesize poly(styrene-*b*-2-vinylpyridine) (PS-*b*-P2VP) followed by post-functionalization with 1-ethyl-2-vinylpyridine (see structure in Table 1). Br^- was ion exchanged to TFSI, nonafluoro-1-butanesulfonic acid ($\text{CF}_3(\text{CF}_2)_3\text{SO}_3^-$),³⁴ as well as, iron bromide ($\text{Fe}_3\text{Br}_{10}^-$)³³.

Taton and coworkers³⁵ introduced a new family of PIL block copolymers based on poly(N-vinyl-3-ethylimidazolium bromide) (PVetImBr) and poly(vinyl acetate) (PVAc) by sequential cobalt-mediated radical polymerization (CMRP) (see structure in Table 1). In addition to obtaining PVAc-*b*-PVetImBr diblock copolymers, synthesis of PVAc-*b*-PVetImBr-*b*-PVAc triblock copolymers was achieved by radical coupling of parent diblocks in the presence of coupling agent isoprene. Taton and coworkers³⁶ also produced a similar PIL diblock copolymer with poly(N-vinyl-3-butylimidazolium bromide) (PVBImBr) as the PIL using a commercially available controlling agent.

Ring opening metathesis polymerization (ROMP) has recently been used by Gin and coworkers³⁸ to synthesize a norbornene and alkylimidazolium-based PIL block copolymer with the aid of a Grubbs' first-generation catalyst. Further research from this group yielded the first ABC PIL triblock copolymer, based on norbornene backbones, with alternating hydrophobic–ionic-hydrophilic substituents (see structure in Table 1).³⁷ More recently, Nishide and coworkers⁴¹ used ROMP and a Grubbs' third-generation catalyst to yield a norbornene-based PIL block copolymer with a redox-active block and an ethylimidazolium-containing PIL block.

Atom transfer radical polymerization (ATRP) is another relatively popular route to produce PIL block copolymers.⁴³⁻⁴⁷ Segalman and coworkers⁴³ synthesized poly(styrene-*b*-histamine methacrylamide) (PS-*b*-PHMA) diblock copolymers *via* ATRP using the activated ester strategy, followed by post-functionalization with trifluoroacetic acid (TFA) resulting in the protic diblock copolymer, PS-*b*-PIL (see structure in Table 1). More recently, ATRP was utilized by Matyjaszewski and coworkers⁴⁶ to produce ABA PIL triblock copolymers with either polyketone (PEEK) or polysulfone (PAES) center blocks and butylimidazolium-containing PIL outer blocks. An ABA PIL triblock copolymer was also synthesized by Tenhu and coworkers⁴⁷ with a poly(*N*-isopropyl acrylamide) (PNIPAm) center block and styrenic outer blocks functionalized with methylimidazole.

2.2. Solid-State Conductivity-Morphology Properties for Electrochemical Energy

Block copolymers are known to self-assemble into a wide range of nanostructured morphologies based on the incompatibility between the different polymers that are covalently attached to one another. For PIL block copolymers in the solid-state, these self-assembled morphologies result in robust films that can accelerate the transport of ions and small molecules

within continuous PIL nanostructured channels. The PIL chemistry within these channels offers unique physiochemical property advantages, such as high electrochemical stability for specific ions (*e.g.* hydroxide, lithium). The transport of these ions is of particular interest as it applies to PIL block copolymers as electrolyte separators in membrane-based alkaline fuel cells and solid-state lithium ion batteries. Although the fuel cell and battery performance has been demonstrated with block copolymers and PILs as the solid-state electrolyte separator,⁵⁰⁻⁵⁷ there have been no papers to date that show fuel cell or battery performance with a PIL block copolymer. Since PIL block copolymers conjoin the properties of both PILs and block copolymers, future fuel cells and batteries containing this material will be of high interest. Here, we highlight findings with regard to conductivity-morphology relationships in solid-state PIL block copolymers as these properties apply to alkaline fuel cell and lithium-ion battery performance.

2.2.1. Water-assisted ion transport (Membrane-based alkaline fuel cells)

Alkaline fuel cells (AFCs) that employ solid-state anion exchange membranes (AEMs) as the electrolyte separator are of great interest as they produce high power densities at low operating temperatures (< 200 °C) and enable the use of non-platinum electrodes (*e.g.*, nickel), significantly reducing cost relative to proton exchange membrane fuel cells.⁵⁸ One critical challenge limiting the wide scale use of membrane-based AFCs is the alkaline stability of polymers used as AEMs. Recently, PIL block copolymers with a range of chemically stable heterocyclic cations have become candidates to investigate for AFCs.^{13, 18, 19, 25, 31, 32}

For AFCs, solid-state single ion conductor PIL block copolymer films that conduct hydroxide anions (OH⁻) under wet conditions are of interest. Additionally, other model hydrophilic mobile anions (*e.g.*, Br⁻, Cl⁻) have been investigated. The transport of hydrophilic anions in PIL block

copolymers is dictated by a water-assisted process, where the conductivity is a strong function of water content and follows an Arrhenius behavior as a function of temperature.^{13, 18, 19, 25, 30, 31}

Elabd, Winey, and coworkers^{18, 19} evaluated the Br⁻ and OH⁻ conductivity of methacrylate-based, butylimidazolium containing PIL block copolymers, poly(MMA-*b*-MEBIm-Br) and poly(MMA-*b*-MEBIm-OH), over a range of PIL compositions. At a fixed PIL composition of 17.3 mol%, the Br⁻ and OH⁻ conductivity of PIL block copolymer was an order of magnitude higher than its analogous PIL random copolymer (at the same PIL composition and water content). The difference in conductivity was attributed to the strong microphase separated lamellar morphology in the PIL block copolymer, where no microphase separation was observed in the PIL random copolymer. The Br⁻ and OH⁻ conductivity of the PIL copolymer was also higher than the PIL homopolymer (control) (shown in Figure 1) at the same experimental conditions, even though the homopolymer possessed a higher PIL composition (100 mol%) and a 2-fold higher water content compared to the block copolymer. These results were unique and suggest that PIL microdomains accelerate water-assisted ion transport compared to bulk PIL homopolymers. Similar results were observed at other PIL compositions (11.9 and 26.5 mol%) as well.¹⁹ Both morphology factor analysis and percolation theory corroborated with the absolute conductivity results and the hypothesis that the local confinement of ions and water in PIL microdomains enhances conductivity.

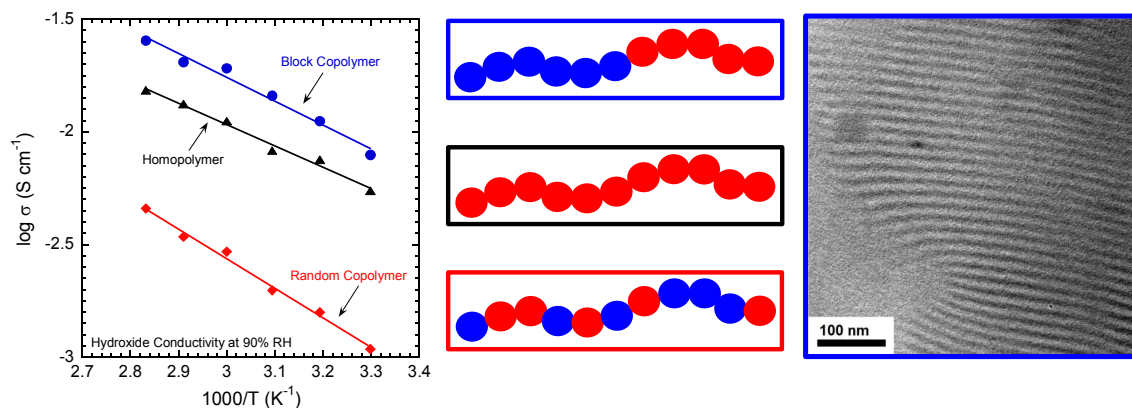


Figure 1. PIL block copolymer, PIL homopolymer, PIL random copolymer from ref. [18]: (left) hydroxide conductivity, (middle) illustration of polymer chain architectures, (right) transmission electron micrograph of PIL block copolymer. Figure adapted from ref. [18].

Elabd and coworkers³¹ investigated a similar PIL block copolymer with a longer alkyl spacer chain between the tethered imidazolium cation and the methacrylate backbone (11 carbon chain versus 2 carbon chain from previous study). Similarly, a high Br⁻ conductivity was measured, which was 3-fold higher than its analogous PIL homopolymer and an order of magnitude higher than the shorter-chain PIL block copolymer from the previous studies despite similar chemistry, similar IEC, similar morphology, and higher water content (shown in Figure 2).

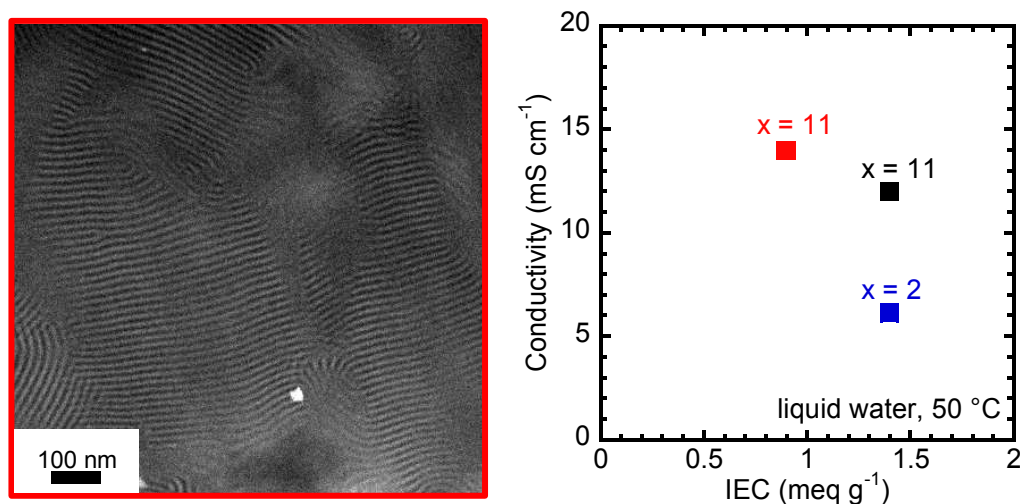


Figure 2. PIL block copolymers from refs. [18, 19, 31, 32] comparing long ($x=11$) and short ($x=2$) alkyl spacer chain lengths between imidazolium and backbone: (left) transmission electron micrograph, (right) bromide ion conductivity. Figure adapted from ref. [32].

Balsara and coworkers¹³ used NMP to produce butylimidazolium- and trimethylammonium-functionalized PIL diblock copolymers over a range of molecular weights and volume fractions. Lamellar morphology was obtained for both bound cations at all volume fractions; domain size of the imidazolium polymer was slightly larger, while the scaling of domain size with chain length showed weak dependency on the nature of the bound cation. Overall, the choice of bound cation had limited effect on the self-assembly, water uptake, and ionic conductivity of the PIL block copolymers. Cl^- conductivity of the membranes was measured in liquid water as a function of temperature (from 25 to 40 °C), and was found to be $\sim 10^{-2} \text{ S cm}^{-1}$ for both cations at higher temperature, although the imidazolium AEM took longer to equilibrate. OH^- conductivity was also measured and was higher than Cl^- conductivity. Similar results were obtained by Elabd and coworkers, where OH^- conductivity exceeded Br^- conductivity.

Balsara and coworkers³⁰ also produced diblock copolymers of the precursor poly(styrene-*b*-bromoethyl acrylate) *via* RAFT and post-functionalized with a tributylphosphonium cation; overall molecular weights ranged from 31 to 87 kg/mol with a fixed volume fraction of the PIL block of ~0.57. These PIL block copolymers self-assembled into lamellar morphologies with domain sizes increasing with molecular weight. Br⁻ ion conductivity and water uptake were measured in samples equilibrated in liquid water; conductivity increased 3-fold with a 2-fold increase in domain size, while water uptake was unaffected by domain size. Overall, high conductivity at relatively low water uptake was achieved as a result of the butyl substituents on the pendant phosphonium cations, which provided a somewhat hydrophobic nature to the cation.

2.2.2. Dry ion transport (Lithium-ion batteries)

Replacing liquid-based electrolytes with solid-state polymer electrolytes (SPEs) can alleviate safety and stability concerns, while in turn offering desirable properties, such as thin-film forming ability, flexibility, and transparency.⁵⁹ The ideal SPE for a solid-state battery would have the high ionic conductivity of a liquid (for high overall storage capacity/energy density), mechanical properties of a solid (for improved stability and cyclability), and the formability of a thermoplastic (for good processability). One proposed strategy is the use of block copolymers as SPEs for lithium ion batteries; one of the block components can solvate (*i.e.*, dissolve) lithium salt to provide a continuous, nanoscopic, ion-conductive pathway, while the other block component provides mechanical rigidity in an ordered nanostructured morphology. Therefore, lithium ion conductive block copolymers conjoin the desired multicomponent properties of high ionic conductivity, robust mechanical properties, and good film forming properties, within a unique nanoscale morphology.^{51, 53, 60-62}

Interestingly, PIL microdomains in PIL block copolymers possess high electrochemical stability in contrast to neutral block copolymers, which has implications for SPEs in lithium-ion batteries.^{14-16, 24, 25, 27, 43} To date, the focus of the ion conductivity studies in PIL block copolymers for this application has focused on fluorinated counter anions (*e.g.*, TFSI⁻, PF₆⁻, BF₄⁻) and not systems that contain lithium salt. However, many common lithium salts used in SPEs are compatible with imidazolium salts and therefore systems with added lithium salt represent an area for future exploration. Typically, when the counter anions in a PIL are fluorinated, this results in a hydrophobic polymer, where ion transport is dictated by the segmental dynamics of the polymer chains (Vogel-Fulcher-Tammann (VFT) behavior).⁵

Mahanthappa and coworkers¹⁴ functionalized a series of poly(styrene-*b*-4-vinylbenzyl chloride) precursors at various compositions (2.7-17.0 mol%) using NMP and subsequently post-functionalized with alkylimidazolium (methyl, butyl, hexyl) cations followed by ion exchange with TFSI⁻ anions. These PIL block copolymers microphase separated into various morphologies: cylinders, lamellae, and coexistence of cylinders and lamellae with varying degrees of long-range order depending on composition and film preparation technique. TFSI⁻ conductivity was highly dependent on PIL composition, morphology type, and degree of long-range order. Specifically, a single PIL block copolymer at 8.6 mol% PIL composition exhibited an order of magnitude difference in conductivity when comparing two different film processing techniques (solvent cast versus melt pressing) resulting from differences in long-range ordered morphologies. Morphology factors (conductivity normalized by PIL homopolymer conductivity and block copolymer PIL volume fraction) approached 0.6 for lamellar samples. Overall, these results indicated the importance of PIL microdomain connectivity and long range ordered morphologies as it relates to ion conductivity.

Long and coworkers¹⁶ reported on a PIL ABA triblock copolymer synthesized *via* NMP with styrene end blocks and a styrenic imidazolium functionalized mid-block with TFSI⁻ anions. Films with a modulus of 100 MPa were achieved and conductivity followed a VFT behavior with temperature. Conductivity approaching 20 mS/cm at 150 °C was achieved when 40 wt% IL was added to the films. A microphase separated morphology without long-range order was measured. Wang and coworkers²⁴ synthesized PIL ABA triblock copolymers with a fluorinated mid-block of poly(vinylidene fluoride-co-hexafluoropropylene) and methacrylate-based imidazolium end blocks over a range of molecular weights and compositions. No microphase separation was observed due to the compatibility of between the PIL with fluorinated anions and the fluoropolymer mid-block. Temperature-dependent conductivity scaled with VFT behavior and the conductivity of TFSI⁻ was higher than BF₄⁻ due to faster polymer chain segmental dynamics (*i.e.*, lower glass transition temperature (T_g)).

Elabd, Winey, and coworkers²⁵ synthesized a series of PIL diblock copolymers *via* RAFT polymerization with methyl methacrylate (MMA) blocks and methacrylate imidazolium-based PIL blocks with TFSI⁻ counter anions at various PIL compositions. The ionic conductivities of the PIL block copolymers were approximately 2 orders of magnitude higher than their analogous PIL random copolymers at similar PIL compositions. The PIL block copolymers exhibited weakly microphase-separated morphologies with no evident long-range periodic structure, while the PIL random copolymers revealed no microphase separation. The higher conductivity in the block copolymers was attributed to the microphase-separated morphology, as significant differences in conductivity were still observed even when differences in glass transition temperature were considered. Interestingly, strong-microphase separated morphology was not a requirement for significant enhancements in conductivity, suggesting that local confinement and

connectivity of nanoscale ionic domains in PIL block copolymers also impact conductivity. Contrastingly, Elabd, Winey, and coworkers²⁷ compared these results to a strong microphase-separated PIL diblock copolymer with styrene (S) and acrylate imidazolium-based PIL blocks at various PIL compositions. At comparable PIL composition, the S-based PIL block copolymer with strong microphase separation exhibited ~ 1.5 – 2 orders of magnitude higher ionic conductivity than the MMA-based PIL block copolymer with weak microphase separation. Similar to the results shown by the Mahanthappa and coworkers¹⁴, various morphology types were observed as a function of PIL content: hexagonally packed cylinders, lamellae, coexisting lamellae and network. Conductivity increased with PIL content, as morphology transitioned from 1-D hexagonally packed cylinders to 2-D lamellae to a coexisting 2-D lamellae and 3-D continuous network (see Figure 3). Morphology types, and subsequently conductivity of these solution-cast membranes, were also found to be dependent on the solvent casting conditions. Overall, the strongly segregated S-based PIL block copolymers exhibited improved transport properties over the PMMA-based PIL block copolymers signifying the impact of the strength of microphase separation on conductivity.

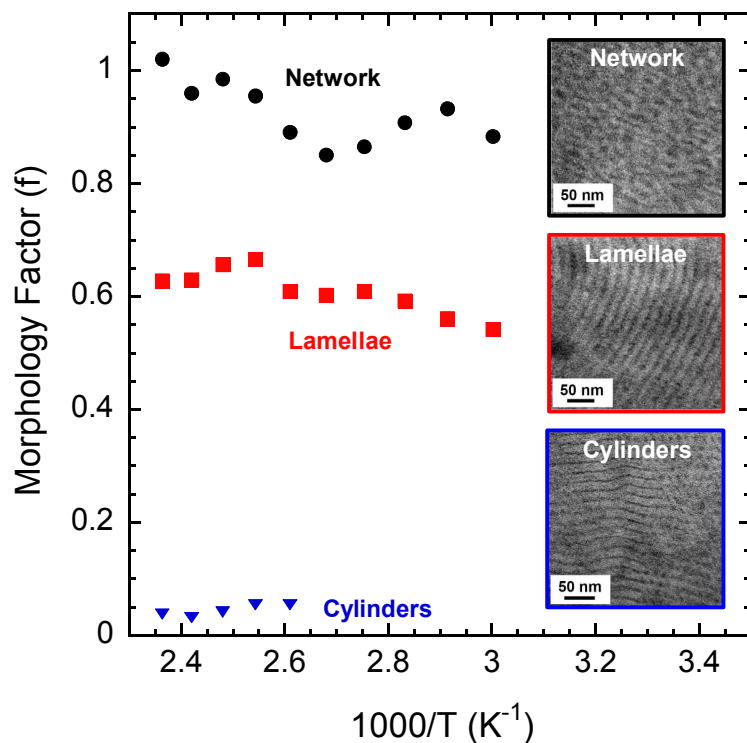


Figure 3. Temperature-dependent morphology factor (normalized ionic conductivity) of PIL diblock copolymers from ref. [27]. Figure adapted from ref. [27].

Segalman and coworkers⁴³ used ATRP to synthesize poly(styrene-block-histamine methacrylamide), PS-*b*-PHMA, which was subsequently treated with trifluoroacetic acid (TFA) to form a protic PIL diblock copolymer. Hexagonally packed cylindrical morphologies were observed for 8 to 20 wt% PHMA, whereas lamellar morphologies were observed in samples containing 32 to 54 wt% PHMA; domain size increased 20-30% with the addition of TFA. Conductivity of the PIL diblock copolymer increased with increasing microdomain channel size (see Figure 4), an atypical result, as usually only volume fraction of conducting domains directly affects conductivity. This result suggests that reduced domain size may hinder ion mobility.

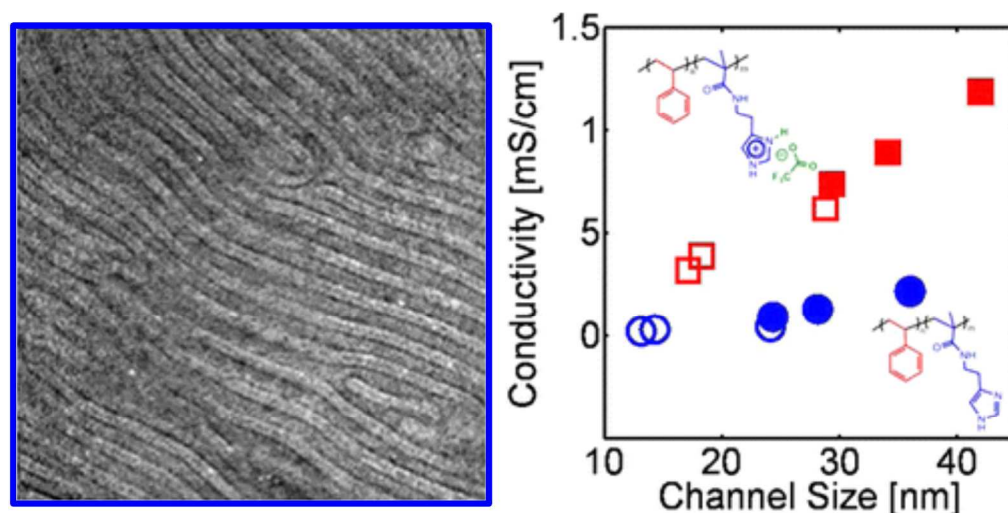


Figure 4. (left) Transmission electron micrograph and (right) conductivity versus microdomain channel size of PIL diblock copolymers (squares) and non-ionic precursor diblock copolymers (circles) from ref. [43]. Open and closed symbols refer to 33 and 53 wt% of PHMA block, respectively. Figure adapted from ref. [43].

Conclusions and Future Directions

Although PIL block copolymers are a relatively new set of block copolymers, researchers have already demonstrated that they can be synthesized from a variety of polymerization techniques, *e.g.*, NMP, RAFT, CMRP, ROMP, ATRP, anionic. Furthermore, PIL block copolymers can be produced either from the direct copolymerization of an IL monomer and a non-ionic monomer or by post-modification of a neutral precursor block copolymer. The versatility in synthesis allows for the inclusion of numerous cations and anions, as well as a broad range of molecular weights and compositions. The careful selection of these parameters results in PIL block copolymer where the morphology and ionic conductivity can be tailored in the solid-state; this has been of high interest lately as it relates to developing electrolyte separators for alkaline fuel cells and lithium-ion batteries. For work focused on water-assisted ion transport (*e.g.*, OH^- , Br^- , Cl^-) for

alkaline fuel cells, microphase separated morphology of the PIL block copolymer allows the conductivity to exceed that of its analogous PIL random copolymer,¹⁸ as well as its analogous PIL homopolymer,^{18, 19, 31} owing to increased transport as a result of ion confinement in PIL nanochannels. Increases in conductivity have been achieved by increasing the size of the conducting channel in lamellar domains, indicating that narrower domains may hinder ion mobility, as well as by the inclusion of hydrophobic long alkyl chains between the cation and backbone or as substituents off the cation.³⁰⁻³² For work focused on dry fluorinated anion transport (*e.g.*, TFSI, BF₄⁻) for lithium-ion batteries, the morphology type, extent of long-range order, strength of microphase separation, processing conditions, and glass transition temperature of the PIL have all been shown to have a significant impact on ion conductivity in PIL block copolymers. Network morphology resulted in increased conductivity relative to lamellae,²⁷ while PIL block copolymers with hexagonally packed cylindrical morphologies exhibited poor ionic conductivity potentially due to increased defects and grain boundaries.^{14, 27} Increasing long-range order through processing conditions was shown to improve ion conductivity.^{14, 27} Faster segmental chain motion, and in turn higher conductivity, was achieved through a lower T_g in the PIL microdomain.²⁴

In summary, the work described here highlights the substantial interest in PIL block copolymers as material components in electrochemical energy devices. Specifically, the future opportunity to explore a richer set of chemistries and therefore properties for PIL block copolymers is promising. Numerous chain sequences (*e.g.*, AB, ABA, ABC, ABCBA), monomers, functional groups and cation/anion combinations can be considered, all leading to a larger set of block copolymers with unique PIL properties to be explored. Note, to date, most PIL block copolymers contain imidazolium as the cation, though there are many more cations in the

IL family. Therefore, in the future, PIL block copolymers with different covalently attached cations will be of interest. Specifically, it is this vast set of cation/anion combinations in ILs that provides a unique opportunity to synthesize numerous PIL block copolymers where many properties can be significantly altered with subtle chemical changes, *e.g.*, mechanical properties, hydrophilicity, ion conductivity, morphology (morphology type, long-range order, strength of microphase separation). Additionally, the demonstration of new PIL block copolymers as separators in fuel cells and batteries provides a new opportunity in electrochemical energy.

Acknowledgements

This work is supported in part by the U.S. Army Research Office under grant no. W911NF-14-0310.

Notes and references

1. T. Welton, *Chemical Reviews*, 1999, **99**, 2071-2083.
2. P. Walden, *Bulletin of the Russian Academy of Sciences*, 1914, 405-422.
3. M. Armand, F. Endres, D. R. MacFarlane, H. Ohno and B. Scrosati, *Nature Materials*, 2009, **8**, 621-629.
4. H. Ohno and K. Ito, *Chemistry Letters*, 1998, 751-752.
5. Y. Ye and Y. A. Elabd, *Polymer*, 2011, **52**, 1309-1317.
6. O. Green, S. Grubjesic, S. Lee and M. A. Firestone, *Polymer Reviews*, 2009, **49**, 339-360.
7. N. Nishimura and H. Ohno, *Polymer*, 2014, **55**, 3289-3297.
8. J. Yuan, D. Mecerreyes and M. Antonietti, *Prog Polym Sci*, 2013, **38**, 1009-1036.
9. D. Mecerreyes, *Prog Polym Sci*, 2011, **36**, 1629-1648.
10. J. Yuan and M. Antonietti, *Polymer*, 2011, **52**, 1469-1482.
11. C. M. Stancik, A. R. Lavoie, J. Schutz, P. A. Achurra, P. Lindner, A. P. Gast and R. M. Waymouth, *Langmuir*, 2004, **20**, 596-605.
12. C. M. Stancik, A. R. Lavoie, P. A. Achurra, R. M. Waymouth and A. P. Gast, *Langmuir*, 2004, **20**, 8975-8987.
13. G. Sudre, S. Inceoglu, P. Cotanda and N. P. Balsara, *Macromolecules*, 2013, **46**, 1519-1527.
14. R. L. Weber, Y. Ye, A. L. Schmitt, S. M. Banik, Y. A. Elabd and M. K. Mahanthappa, *Macromolecules*, 2011, **44**, 5727-5735.

15. S. Cheng, F. L. Beyer, B. D. Mather, R. B. Moore and T. E. Long, *Macromolecules*, 2011, **44**, 6509-6517.
16. M. D. Green, D. Wang, S. T. Hemp, J.-H. Choi, K. I. Winey, J. R. Heflin and T. E. Long, *Polymer*, 2012, **53**, 3677-3686.
17. X. Li, X. Ni, Z. Liang and Z. Shen, *Journal of Polymer Science Part A: Polymer Chemistry*, 2012, **50**, 2037-2044.
18. Y. Ye, S. Sharick, E. M. Davis, K. I. Winey and Y. A. Elabd, *Acs Macro Letters*, 2013, **2**, 575-580.
19. K. M. Meek, S. Sharick, Y. Ye, K. I. Winey and Y. A. Elabd, *Macromolecules*, 2015, **48**, 4850-4862.
20. J. Yang, W. L. Sun, W. H. Lin and Z. Q. Shen, *J Polym Sci Pol Chem*, 2008, **46**, 5123-5132.
21. K. Vijayakrishna, S. K. Jewrajka, A. Ruiz, R. Marcilla, J. A. Pomposo, D. Mecerreyes, D. Taton and Y. Gnanou, *Macromolecules*, 2008, **41**, 6299-6308.
22. H. Mori, M. Yahagi and T. Endo, *Macromolecules*, 2009, **42**, 8082-8092.
23. J. Yuan, H. Schlaad, C. Giordano and M. Antonietti, *Eur Polym J*, 2011, **47**, 772-781.
24. C. Chanthad, K. A. Masser, K. Xu, J. Runt and Q. Wang, *J Mater Chem*, 2012, **22**, 341-344.
25. Y. Ye, J.-H. Choi, K. I. Winey and Y. A. Elabd, *Macromolecules*, 2012, **45**, 7027-7035.
26. Z. Wang, H. Lai and P. Wu, *Soft Matter*, 2012, **8**, 11644-11653.
27. J.-H. Choi, Y. Ye, Y. A. Elabd and K. I. Winey, *Macromolecules*, 2013, **46**, 5290-5300.
28. E. Karjalainen, N. Chenna, P. Laurinmaki, S. J. Butcher and H. Tenhu, *Polym Chem-Uk*, 2013, **4**, 1014-1024.
29. B. J. Adzima, S. R. Venna, S. S. Klara, H. He, M. Zhong, D. R. Luebke, M. S. Mauter, K. Matyjaszewski and H. B. Nulwala, *J Mater Chem A*, 2014, **2**, 7967-7972.
30. P. Cotanda, G. Sudre, M. A. Modestino, X. C. Chen and N. P. Balsara, *Macromolecules*, 2014, **47**, 7540-7547.
31. J. R. Nykaza, Y. Ye and Y. A. Elabd, *Polymer*, 2014, **55**, 3360-3369.
32. J. R. Nykaza, Y. Ye, R. Nelson, A. C. Jackson, F. L. Beyer, E. M. Davis, K. Page, S. Sharick, K. I. Winey and Y. A. Elabd, *Unpublished*.
33. P. M. Carrasco, L. Tzounis, F. J. Mompean, K. Strati, P. Georgopoulos, M. Garcia-Hernandez, M. Stamm, G. Cabanero, I. Odriozola, A. Avgeropoulos and I. Garcia, *Macromolecules*, 2013, **46**, 1860-1867.
34. P. M. Carrasco, A. R. de Luzuriaga, M. Constantinou, P. Georgopoulos, S. Rangou, A. Avgeropoulos, N. E. Zafeiropoulos, H.-J. Grande, G. Cabanero, D. Mecerreyes and I. Garcia, *Macromolecules*, 2011, **44**, 4936-4941.
35. C. Detrembleur, A. Debuigne, M. Hurtgen, C. Jerome, J. Pinaud, M. Fevre, P. Coupillaud, J. Vignolle and D. Taton, *Macromolecules*, 2011, **44**, 6397-6404.
36. P. Coupillaud, M. Fevre, A.-L. Wirotius, K. Aissou, G. Fleury, A. Debuigne, C. Detrembleur, D. Mecerreyes, J. Vignolle and D. Taton, *Macromolecular rapid communications*, 2014, **35**, 422-430.
37. E. F. Wiesenauer, N. Phuc Tien, B. S. Newell, T. S. Bailey, R. D. Noble and D. L. Gin, *Soft Matter*, 2013, **9**, 7923-7927.
38. E. F. Wiesenauer, J. P. Edwards, V. F. Scalfani, T. S. Bailey and D. L. Gin, *Macromolecules*, 2011, **44**, 5075-5078.

39. V. F. Scalfani, E. F. Wiesenauer, J. R. Ekblad, J. P. Edwards, D. L. Gin and T. S. Bailey, *Macromolecules*, 2012, **45**, 4262-4276.
40. P. T. Nguyen, E. F. Wiesenauer, D. L. Gin and R. D. Noble, *J Membrane Sci*, 2013, **430**, 312-320.
41. T. Suga, M. Sakata, K. Aoki and H. Nishide, *ACS Macro Letters*, 2014, **3**, 703-707.
42. D. V. Krogstad, S.-H. Choi, N. A. Lynd, D. J. Audus, S. L. Perry, J. D. Gopez, C. J. Hawker, E. J. Kramer and M. V. Tirrell, *The Journal of Physical Chemistry B*, 2014, **118**, 13011-13018.
43. Y. Schneider, M. A. Modestino, B. L. McCulloch, M. L. Hoarfrost, R. W. Hess and R. A. Segalman, *Macromolecules*, 2013, **46**, 1543-1548.
44. J. Texter, V. A. Vasantha, R. Crombez, R. Maniglia, L. Slater and T. Mourey, *Macromolecular Rapid Communications*, 2012, **33**, 69-74.
45. Z. Shi, B. S. Newell, T. S. Bailey and D. L. Gin, *Polymer*, 2014, **55**, 6664-6671.
46. N. A. Agudelo, A. M. Elsen, H. He, B. L. López and K. Matyjaszewski, *Journal of Polymer Science Part A: Polymer Chemistry*, 2015, **53**, 228-238.
47. E. Karjalainen, V. Khlebnikov, A. Korpi, S.-P. Hirvonen, S. Hietala, V. Aseyev and H. Tenhu, *Polymer*, 2015, **58**, 180-188.
48. N. D. Hann, *Journal of Polymer Science: Polymer Chemistry Edition*, 1977, **15**, 1331-1339.
49. A. Domard, M. Rinaudo and C. Rochas, *J Polym Sci Polym Phys Ed*, 1979, **17**, 673-681.
50. A. N. Lai, L. S. Wang, C. X. Lin, Y. Z. Zhuo, Q. G. Zhang, A. M. Zhu and Q. L. Liu, *Acs Appl Mater Inter*, 2015, **7**, 8284-8292.
51. P. E. Trapa, B. Huang, Y.-Y. Won, D. R. Sadoway and A. M. Mayes, *Electrochemical and solid-state letters*, 2002, **5**, A85-A88.
52. R. Bouchet, S. Maria, R. Meziane, A. Aboulaich, L. Lienafa, J.-P. Bonnet, T. N. Phan, D. Bertin, D. Gigmes and D. Devaux, *Nature materials*, 2013, **12**, 452-457.
53. P. P. Soo, B. Huang, Y. I. Jang, Y. M. Chiang, D. R. Sadoway and A. M. Mayes, *J Electrochem Soc*, 1999, **146**, 32-37.
54. K. Yin, Z. Zhang, X. Li, L. Yang, K. Tachibana and S.-i. Hirano, *J Mater Chem A*, 2015, **3**, 170-178.
55. R. Bouchet, S. Maria, R. Meziane, A. Aboulaich, L. Lienafa, J.-P. Bonnet, T. N. T. Phan, D. Bertin, D. Gigmes, D. Devaux, R. Denoyel and M. Armand, *Nat Mater*, 2013, **12**, 452-457.
56. M. Li, L. Yang, S. Fang, S. Dong, S. i. Hirano and K. Tachibana, *Polymer International*, 2012, **61**, 259-264.
57. M. Li, B. Yang, L. Wang, Y. Zhang, Z. Zhang, S. Fang and Z. Zhang, *J Membrane Sci*, 2013, **447**, 222-227.
58. J. R. Varcoe and R. C. T. Slade, *Fuel Cells*, 2005, **5**, 187-200.
59. J. Song, Y. Wang and C. Wan, *J Power Sources*, 1999, **77**, 183-197.
60. A. Panday, S. Mullin, E. D. Gomez, N. Wanakule, V. L. Chen, A. Hexemer, J. Pople and N. P. Balsara, *Macromolecules*, 2009, **42**, 4632-4637.
61. E. D. Gomez, A. Panday, E. H. Feng, V. Chen, G. M. Stone, A. M. Minor, C. Kisielowski, K. H. Downing, O. Borodin and G. D. Smith, *Nano Lett*, 2009, **9**, 1212-1216.
62. M. Singh, O. Odusanya, G. M. Wilmes, H. B. Eitouni, E. D. Gomez, A. J. Patel, V. L. Chen, M. J. Park, P. Fragouli and H. Iatrou, *Macromolecules*, 2007, **40**, 4578-4585.

